Available online at www.sciencedirect.com
SCIENCE DIRECT
Journal of Photochemistry and Photobiology A: Chemistry 178 (2006) 140–149
Journal of Photochemistry and Photobiology A:Chemistry
www.elsevier.com/locate/jphotochem

Two-photon absorption properties of conjugated supramolecular porphyrins with electron donor and acceptor

Junichi Tanihara, Kazuya Ogawa, Yoshiaki Kobuke *

Graduate School of Materials Science, Nara Institute of Science and Technology, 8916-5 Takayama, Ikoma, Nara 630-0101, Japan

Available online 6 December 2005

Abstract

Two-photon absorption (2PA) cross-section values of supramolecular porphyrin tetramer consisting of two monoacetylene-linked bisporphyrins with and without ferrocene/C_{60} groups as electron donor/acceptor through the coordination of pyridyl to zinc were measured using a nanosecond open aperture Z-scan method. The maximum effective cross-section value was observed for the compound having asymmetric terminals of ferrocene and C_{60} as 2.0×10^5 GM. The values obtained for compounds having two C_{60}'s, two ferrocene's, no donor/acceptor, and stacked isomer were 1.7×10^5 GM, 1.5×10^5 GM, 1.1×10^5 GM, and 1.3×10^5 GM, respectively. These results indicate that the asymmetric donor–π–acceptor structure is the best for 2PA enhancement for this series of molecules. These values are extremely large compared to those of unit dimer **2D** (190 GM at 780 nm) and compounds reported hitherto in literatures.

Keywords: Porphyrin; Two-photon absorption; Fullerene; Ferrocene; Self-assembly

1. Introduction

Two-photon absorption (2PA) is a non-linear optical phenomenon, which occurs through simultaneous absorption of two photons and has recently been the subject of much interest. Because of quadratic dependence on the incident light intensity in the 2PA process, the efficiency becomes largest at the focal point. Therefore, two-photon excitation is expected to find a variety of optical applications, which include photodynamic therapy [1–3], 3-D optical data storage [4–7], and optical limiting [8]. Although the first prediction of 2PA was made by Maria Göppert–Mayer in 1931 [9] and the first observation was reported in 1961 [10] after introduction of laser technology, this field had not been active because materials with large 2PA cross-section values ($\sigma^{(2)}$) were not discovered. In recent years, new classes of molecules exhibiting large $\sigma^{(2)}$ values have been reported according to the strategies employing donor/acceptor sets with a π-conjugation system in a symmetric (D–π–D or A–π–A) [11] or asymmetric (D–π–A) arrangement [12].

Porphyrin is the promising candidate for 2PA materials because of the highly conjugated π-electron system, but simple monomeric porphyrins without donor/acceptor groups, such as tetraphenylporphyrin (H_2TPP) and zincoctaethylporphyrin (ZnOEP), exhibit only small $\sigma^{(2)}$ values below a few tens of GM ($1\,\mathrm{GM} = 10^{-50}\,\mathrm{cm^4\,s\,molecule^{-1}\,photon^{-1}}$) [13]. Porphyrin derivatives are used for cancer treatment as a photodynamic therapy (PDT) agent. However, visible light in red region limits the penetration depth on the surface due to the absorption by biological tissue. The use of light in the near-infrared (NIR) wavelength from 700 to 1500 nm, a so-called "optical window" for biological tissues [14], is advantageous for better penetration to the tissue. Thus, porphyrins with large $\sigma^{(2)}$ values at the NIR region will allow spatially selective treatment of cancer even at deep sites.

We have reported that zinc complex of *meso*-(*N*-methyl)imidazolylporphyrin like **1** led to the formation of a stable slipped cofacial dimer **2D** by the complementary coordination of imidazolyl to pentacoordinating zinc in non-coordinating solvents with a stability constant over $10^{11}\,\mathrm{M^{-1}}$ [15]. Despite such high stability constant, the dimeric structure can be cleaved by the presence of coordinating solvents such as MeOH and pyridine, and reorganized on eliminating the solvents. This procedure has allowed us to prepare various supramolecular porphyrin architectures [16] such as long linear arrays [17]

* Corresponding author. Tel.: +81 743 72 6110; fax: +81 743 72 6119.
E-mail address: kobuke@ms.naist.jp (Y. Kobuke).

1010-6030/$ – see front matter © 2005 Elsevier B.V. All rights reserved.
doi:10.1016/j.jphotochem.2005.10.042

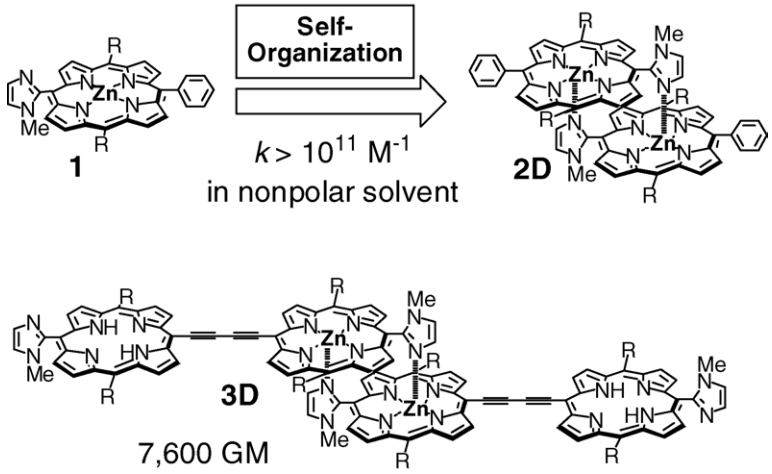

Scheme 1. Formation of self-assembled dimer **2D** and structure of compound **3D**.

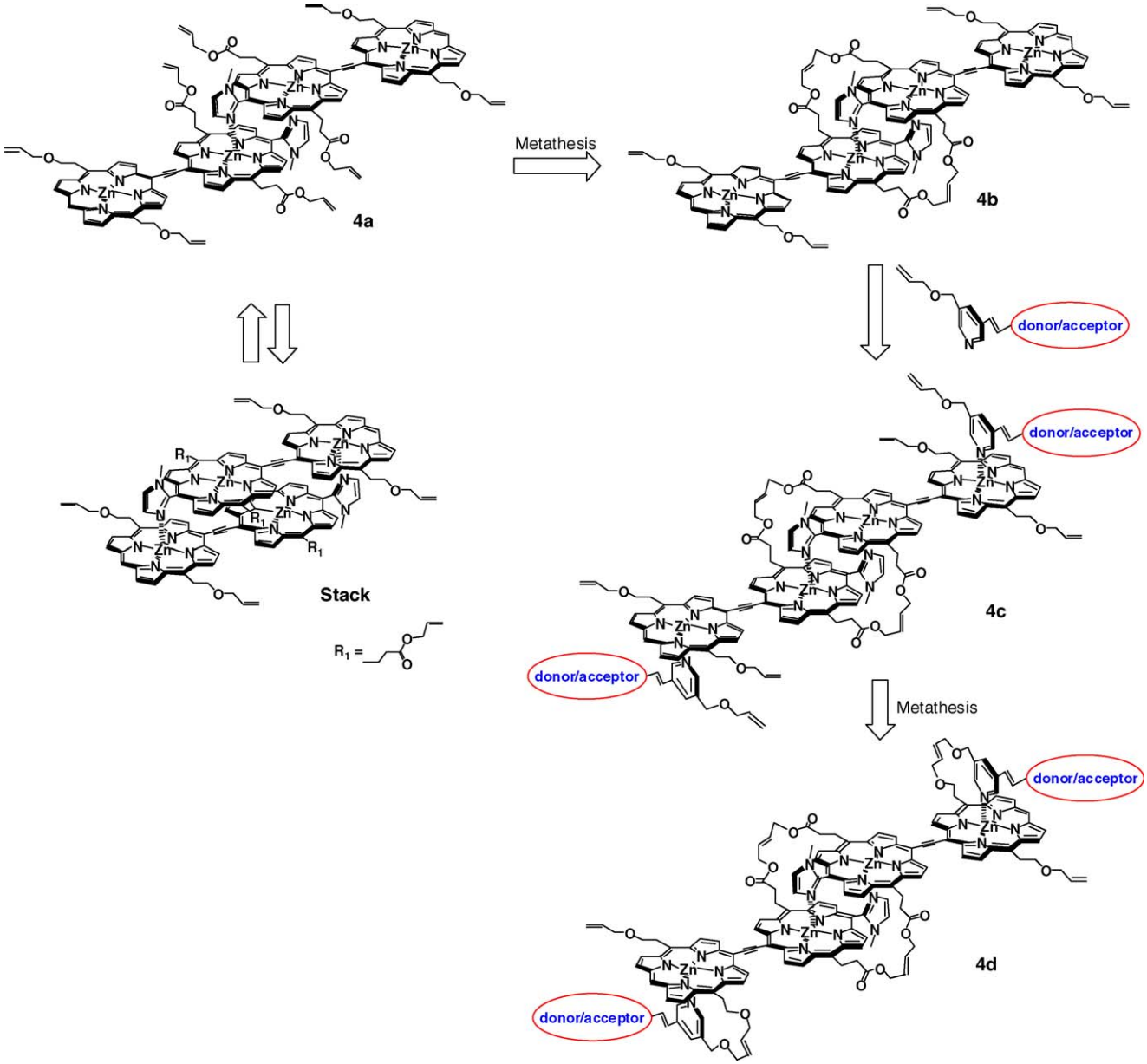

Scheme 2. Strategy for construction of conjugated porphyrin supermolecules with donor and acceptor.

with large third-order optical non-linearity [18] and macrocycles [19] with light-harvesting function mimicking photosynthetic antenna rings (Scheme 1).

Recently, we reported that the self-assembled conjugated porphyrin **3D** exhibited a very large $\sigma^{(2)}$ value (7600 GM), which was the largest among the reported measured by using femtosecond pulses [20]. The large enhancement could be attributed to three factors: (i) extended π-conjugation over two porphyrins by using a bisacetylene link, (ii) molecular polarization induced by the asymmetric donor/acceptor arrangement of zinc- and free base porphyrins and (iii) complementary coordination of imidazolyl to zinc. To gain insights into a further increase of the $\sigma^{(2)}$ value, it is interesting to introduce electron donor and/or acceptor groups to a conjugated imidazolyl porphyrin system in order to polarize further the molecule. If one more zinc ion is inserted into the outside free base porphyrin of the self-assembly **3D**, additional coordination sites become available for connecting donor/acceptor groups through coordinating ligands. According to this idea, we designed a novel conjugated supramolecular porphyrin system as shown in Scheme 2. The designed porphyrin tetramer **4a** has two terminal zincporphyrins as the host of ligands but no terminal imidazolyl group and the formation of self-organized linear polymer is prevented. For facile preparation of asymmetric bisporphyrin units, monoacetylene linking was adopted, where direct hetero-coupling reaction between porphyrins with and without imidazole was undertaken. During the preparation process of **4a**, a coordination isomer named **stack** was gradually formed in a chloroform solution and went back again to **4a** by adding coordinating solvent such as pyridine. In this stacked isomer, each imidazolyl group coordinates to the zinc porphyrin site having no imidazolyl group to give a stack configuration rather than the extended one. In order to prohibit the interconversion of the coordination isomers once obtained, the complementary coordination pair was covalently linked by metathesis reaction [21] to give the tetramer host **4b** that can accept two external ligands at terminal zincporphyrins. As the guest ligand, 3,5-disubstituted pyridine was chosen, in which one subsistent carries an olefinic group for linking to porphyrin by metathesis reaction with one of the olefinic substituents at the *meso*-position, and the other bears an electron donor or acceptor. In this work, ferrocene (Fc) and C_{60} were used as the donor and acceptor, respectively. Thus, three supermolecules **FcFc**, **$C_{60}C_{60}$**, and **C_{60}Fc** (Scheme 3) were prepared by coordination, followed by metathesis connection to give **4d** through **4c**. The details of preparation and structural characterization will be published elsewhere. When the porphyrin part is photo-irradiated, charge separated species should result. In the case of **FcFc**, charge shift from Fc to porphyrin is expected to give the charge separated state, $Fc^{\bullet+}$–$ZnP^{\bullet-}$, while in the case of **$C_{60}C_{60}$**, the charge separated species will be $ZnP^{\bullet+}$–$C_{60}{}^{\bullet-}$. Therefore, **FcFc** and **$C_{60}C_{60}$** may belong to D–A–D and A–D–A configurations, respectively. On the other hand, in the case of **C_{60}Fc**, charge separation will occur first between porphyrin and C_{60} followed by charge shift from Fc to porphyrin cation radical to afford the final charge separated state, $C_{60}{}^{\bullet-}$–ZnP–$Fc^{\bullet+}$, i.e. D–π–A configuration. Such the configuration produced by absorption of the first photon may increase the transition probability of the second photon resulting in large cross-section values.

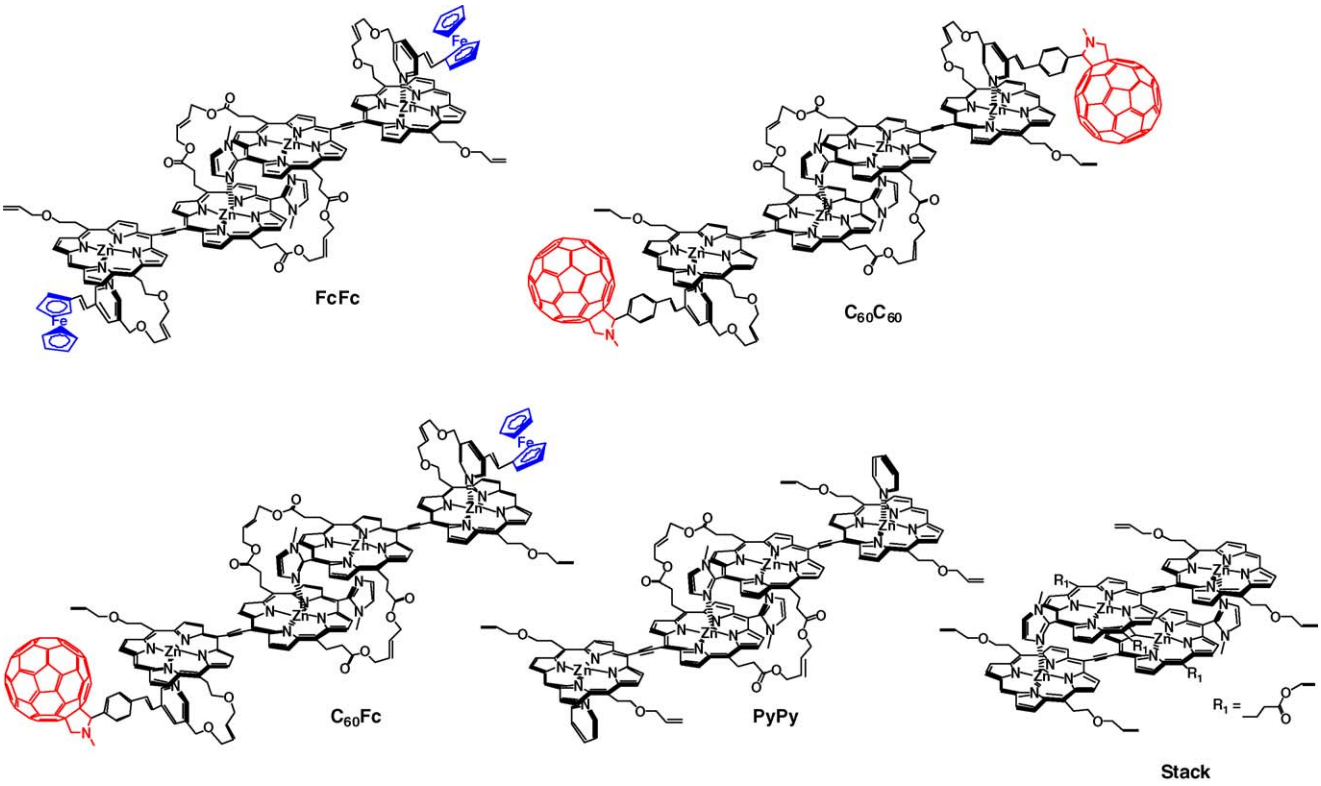

Scheme 3. Structures of porphyrin supermolecules investigated in this study.

In this study, 2PA properties of supramolecular porphyrins were investigated by nanosecond open aperture Z-scan measurements. The porphyrin tetramer without a donor/acceptor but coordinated by pyridine **PyPy**, the stacked isomer **stack**, and coordination dimer **2D** were also measured for comparison.

2. Results and discussion

Fig. 1 shows UV–vis absorption spectra of porphyrins investigated in this work. The complementary coordination dimer **2D** gave split Soret bands at 413 nm and 436 nm. The splitting energy of 1280 cm^{-1} indicates the presence of fairly large exciton interaction between two porphyrins. This can be explained as a result of head-to-tail and face-to-face orientations of two mutually orthogonal transition dipoles in the slipped cofacial arrangement [15,19]. All the other self-assembled acetylene-linked bisporphyrins show further a larger splitting of 4280 cm^{-1} (around at 405 nm and 490 nm). When 10% pyridine was added into the tetrachloroethane solution of **4a** or **stack**, the splitting energy decreased to 2920 cm^{-1} (424 nm and 484 nm) as a result of cleavage of the complementary coordination of imidazolyl to zinc. The splitting energy is contributed from the exciton interactions of face-to-face and head-to-tail transitions of two porphyrins in a π-conjugation and complementary coordination. The significant part of the splitting energy observed in self-assembled tetramers (2920 cm^{-1}) comes from π-conjugated porphyrins [22,23] and another incremental component (1360 cm^{-1}) may be ascribed to the exciton interactions between two bisporphyrin units in the complementary coordination. The effect of increased conjugation reflected in strongly intensified and red-shifted Q-bands around 730 nm. The intensified Q-band is considered to be contributed from the reduced a_{1u}–a_{2u} degeneracy as well as the increased conjugation [24] and to allow large 2PA cross-section values because a resonance enhancement [13,25] of the Q-band may be amplified, too. The self-assemblies bring large extinction coefficients for one-photon absorption around 400–500 nm (S_2 state), but negligible absorption is observed over 800 nm. Therefore, it is expected that two photons in 800–1000 nm region will be absorbed simultaneously to promote the molecule to the S_2 state.

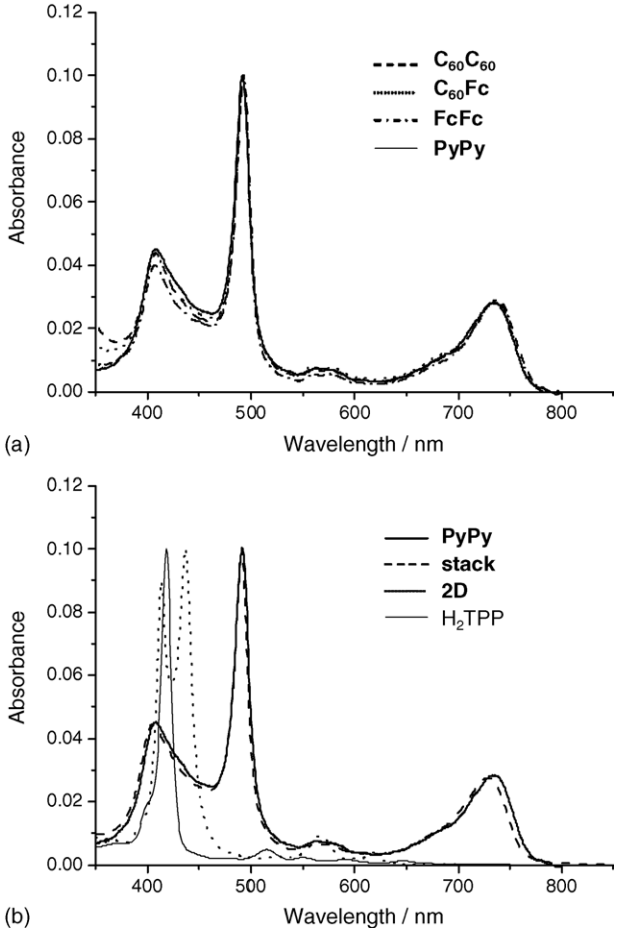

Fig. 1. One-photon absorption spectra of (a) **$C_{60}C_{60}$**, **C_{60}Fc**, **FcFc**, and **PyPy**, and (b) **PyPy**, **stack**, **2D**, and H_2TPP. The solvents used were: tetrachloroethane for **$C_{60}C_{60}$**, **C_{60}Fc**, **FcFc**, and **stack**; tetrachloroethane containing 1% pyridine for **PyPy**; chloroform for **2D** and H_2TPP.

Fig. 2 shows a typical Z-scan trace for **C_{60}Fc** in tatrachloroethane (9 μM, dotted) with a pulse energy of 1 mJ (corresponding to $I_0 = 1.0 \times 10^{14}$ W m^{-2}) and a theoretically fitted curve (solid line). In this figure, the normalized transmittance is plotted as a function of the sample position, z. The large dip was observed around the focal position due to the non-linear absorption. The curve fit was based on the theoretical expression for the transmittance with the following equations [20,26,27]:

$$T(\zeta) = \frac{(1-R)^2\, e^{(-\alpha^{(1)}L)}}{\sqrt{\pi}q(\zeta)} \int_{-\infty}^{\infty} \ln[1 + q(\zeta)\, e^{(-x^2)}]\, dx \quad (1)$$

$$q(\zeta) = \frac{q_0}{1+\zeta^2} \quad (2)$$

$$q_0 = \alpha^{(2)}(1-R) I_0\, L_{\text{eff}} \quad (3)$$

$$L_{\text{eff}} = \frac{[1 - \exp(-\alpha^{(1)}L)]}{\alpha^{(1)}} \quad (4)$$

$$\sigma^{(2)} = \frac{\overline{h}\omega\, \alpha^{(2)}}{N} \quad (5)$$

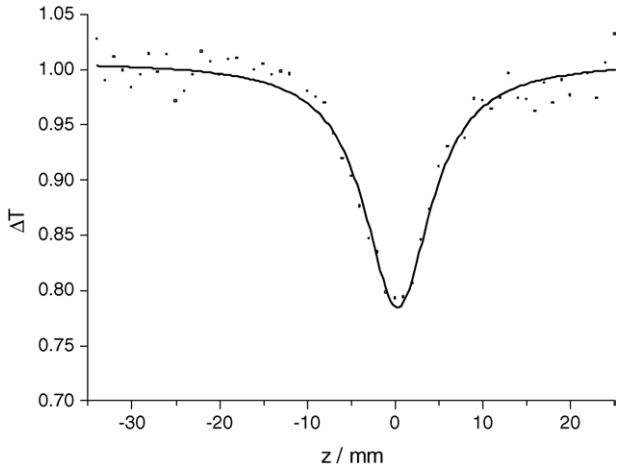

Fig. 2. Typical open-aperture Z-scan traces (dot) of **C_{60}Fc** at 880 nm with pulse energy of 1 mJ corresponding to $I_0 = 1.0 \times 10^{14}$ W m^{-2} with theoretical fitting curves (solid).

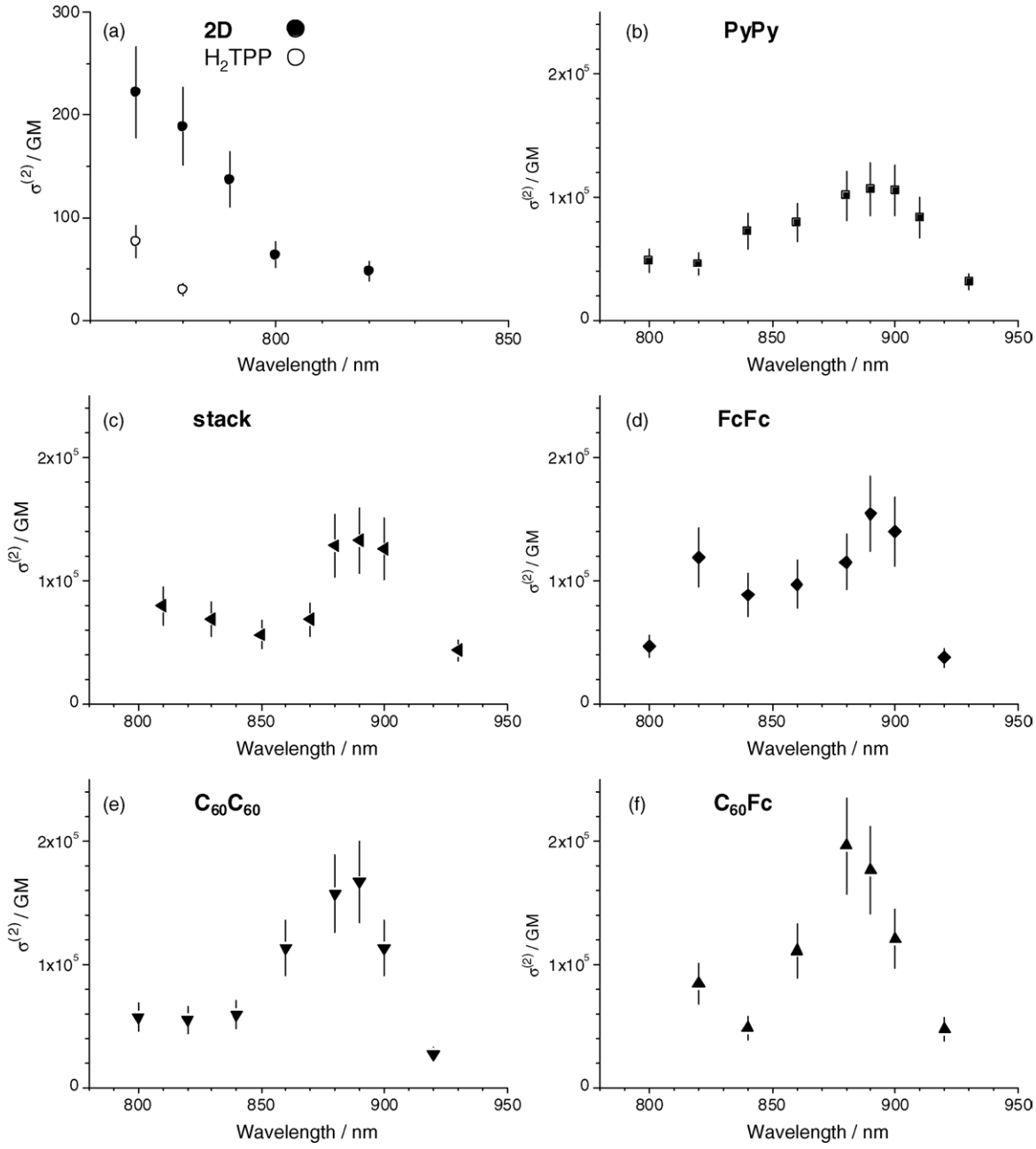

Fig. 3. 2PA spectra of (a) **2D** and H_2TPP, (b) **PyPy**, (c) **stack**, (d) **FcFc**, (e) **$C_{60}C_{60}$**, and (f) **C_{60}Fc**. The solvents used were: tetrachloroethane for **$C_{60}C_{60}$**, **FcFc**, **C_{60}Fc**, and **stack**; tetrachloroethane containing 1% pyridine for **PyPy**; chloroform for **2D** and H_2TPP.

where ζ is the normalized z-position ($\zeta = (z - z_0)/z_R$), and z_0 and z_R the focal position and the Rayleigh range, respectively, $\alpha^{(1)}$ a one-photon absorption coefficient, R denotes the Fresnel reflectance and L is the path length. $\alpha^{(2)}$ is the 2PA coefficient, L_{eff} denotes the effective path length and I_0 is the peak intensity at the focal position. N is the number density of the molecules and $\bar{h}\omega$ is the photon energy of the incident light. Finally, the effective $\sigma^{(2)}$ value was estimated from the Eq. (5).

Plots of effective $\sigma^{(2)}$ values as a function of wavelength (2PA spectra) are shown in Fig. 3. In the cases of H_2TPP and coordination dimer unit **2D**, the cross-sections increased with shortening the wavelength of incident light. Such the behavior was observed in porphyrin monomers such as H_2TPP and ZnOEP measured using a femtosecond fluorescence method and was explained as a resonance enhancement nearby one-photon absorption of the Q-band [13]. The femtosecond data of H_2TPP and ZnOEP in the literature were 15 GM and 4.4 GM, respectively, at 780 nm. The $\sigma^{(2)}$ values of H_2TPP and **2D** measured using nanosecond laser at 780 nm in this study were estimated to be 29 GM and 190 GM (95 GM per porphyrin, see Fig. 3(a) and Table 1), respectively. The value of H_2TPP measured by nanosecond laser is twice of that by femtosecond, indicating that the contribution of excited state absorption (ESA), which is usually observed in nanosecond measurements and the cross-section value is two to three

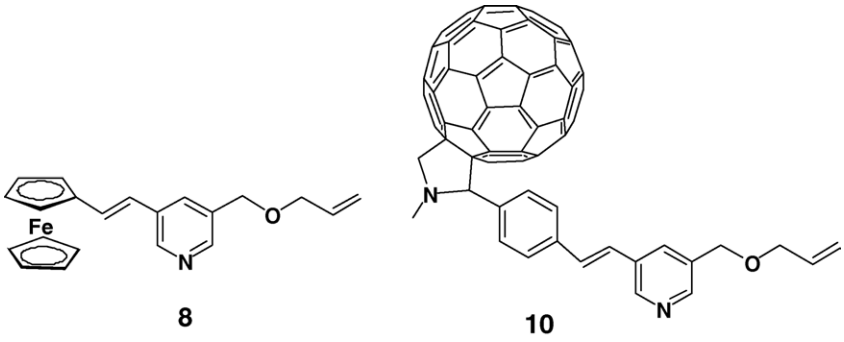

Scheme 4. Structures of compounds **8** and **10**.

orders of magnitude larger than that obtained by femtosecond pulse [28–30], is rather small. Although the value of **2D** per porphyrin is three times larger than that of H_2TPP at 780 nm, it should be noted here that these values are not the maximum and the peaks may lie below 780 nm.

On the other hand, supermolecules consisting of acetylene-linked bisporphyrin exhibited extremely large effective $\sigma^{(2)}$ values at around 880–900 nm as shown in Fig. 3(b–f). In all cases, the one-photon transition energy corresponding to the 2PA maximum (440–450 nm) disagreed with one-photon Soret bands. This suggests that the final 2PA state is *gerade* and electronic structure in tetrameric porphyrin framework is approximately centrosymmetric. The maximum effective $\sigma^{(2)}$ values were estimated to be $(1.1 \pm 0.22) \times 10^5$ ($(2.8 \pm 0.56) \times 10^4$ per porphyrin) GM for **PyPy**, $(1.3 \pm 0.26) \times 10^5$ ($(3.2 \pm 0.64) \times 10^4$ per porphyrin) GM for **stack**, $(1.5 \pm 0.30) \times 10^5$ ($(3.8 \pm 0.76) \times 10^4$ per porphyrin) GM for **FcFc**, $(1.7 \pm 0.34) \times 10^5$ ($(4.3 \pm 0.86) \times 10^4$ per porphyrin) GM for $\mathbf{C_{60}C_{60}}$, and $(2.0 \pm 0.40) \times 10^5$ ($(5.0 \pm 1.0) \times 10^4$ per porphyrin) GM for $\mathbf{C_{60}Fc}$, as summarized in Table 1. These values are three orders of magnitude larger than those obtained for **2D**. This result indicates that the acetylene linkages, irrespective of mono and bis ones, are effective for enhancing significantly the 2PA cross-section (bisacetylene compounds exhibited the same order of magnitude of the effective $\sigma^{(2)}$ values in nanosecond timescale, which will be published elsewhere). On comparing the series of compounds, the magnitude is in the order $\mathbf{C_{60}Fc} > \mathbf{C_{60}C_{60}} > \mathbf{FcFc} > \mathbf{stack} > \mathbf{PyPy}$. This order is correlated with that of the fluorescence quenching efficiency, which corresponds to the efficiency of photo-induced electron transfer, 85% for $\mathbf{C_{60}C_{60}}$, 63% for $\mathbf{C_{60}Fc}$, and 44% for **FcFc** based on the fluorescence intensity of **PyPy**. Despite lower the fluorescence quenching efficiency for $\mathbf{C_{60}Fc}$ than that for $\mathbf{C_{60}C_{60}}$, the order for the cross-section value is reverse to this. This suggests that the asymmetric D–π–A structure contributes more significantly than symmetric D–A–D and A–D–A configurations for the 2PA enhancement. Compounds **8** and **10** (Scheme 4) were measured to investigate the contribution from Fc and C_{60} moieties to the $\sigma^{(2)}$ value, however, no non-linear absorption (∼mM concentration) was observed in the range from 780 nm to 930 nm. Although **stack** exhibited a slightly larger cross-section value (1.3×10^4 GM) than **PyPy**, the difference is not so significant. These results provide a new strategy constructing molecules, where the porphyrin is employed as the central π-system with Fc/C_{60} as a donor/acceptor set to expect large 2PA cross-section values. Although the effective $\sigma^{(2)}$ values reported hitherto through nanosecond pulses were in the range a few GM to 10^5 GM, the values observed in this study are the largest classes in literatures [11,12,28–30]. Such the huge cross-section values will open wide the way to 2PA applications such as PDT and a 3-D data storage device.

Table 1
2PA cross-section values ($\sigma^{(2)}$) of porphyrins

Sample	$\sigma^{(2)}$ (GM; per porphyrin)	Wavelength (nm)	Solvent
H_2TPP	29 (–)	780	$CHCl_3$
2D	190 (95)	780	$CHCl_3$
PyPy	1.1×10^5 (2.8×10^4)	890	TCE + 1% py
stack	1.3×10^5 (3.2×10^4)	890	TCE
FcFc	1.5×10^5 (3.8×10^4)	890	TCE
$\mathbf{C_{60}C_{60}}$	1.7×10^5 (4.3×10^4)	890	TCE
$\mathbf{C_{60}Fc}$	2.0×10^5 (5.0×10^4)	880	TCE

TCE, tetrachloroethane; py, pyridine.

3. Conclusions

In this work, 2PA properties of supramolecular porphyrin system consisting of porphyrin tetramer are investigated. In the supramolecular porphyrin system, π-conjugation between two porphyrins of bisporphyrin unit is expanded by using the monoacetylene linkage and ferrocene/C_{60} groups are attached as donor/acceptor terminals by coordination of external pyridyl ligands to zinc, followed by metathesis linking. The order of the maximum effective cross-section values is $\mathbf{C_{60}Fc}$ (2.0×10^5 GM) > $\mathbf{C_{60}C_{60}}$ (1.7×10^5 GM) > **FcFc** (1.5×10^5 GM) > **stack** (1.3×10^5 GM) > **PyPy** (1.1×10^5 GM). The results suggest that the asymmetric D–π–A structure is advantageous for enhancing the 2PA in this series of molecules. All of these values are extremely large compared to those of dimer **2D** (190 GM at 780 nm). The porphyrin supermolecules investigated here are interesting materials for applications to 2PA-PDT and 3-D optical memory.

4. Experimental

^{1}H and ^{13}C NMR spectra were measured by using a JEOL EX 270 spectrometer. MALDI-TOF mass spectra were measured with Voyager DE-STR (PerSeptive Biosystems) or KRATOS AXIMA using dithranol as a matrix.

4.1. Synthesis of 3-allyloxymethyl-5-hydroxymethyl-pyridine: ***5***

Under a nitrogen atmosphere, 3,5-dihydroxymethylpyridine [31] (16 mmol) and sodium hydride (47 mmol) were added into 140 mL of dry DMF and the mixture was stirred for 1 h at room temperature. Allyl bromide (5.5 mmol) dissolved in dry DMF (10 mL) was added dropwise into the mixture over 15 min. After stirring for 2.5 h, the solvent was removed under vacuum and the residue was extracted with chloroform. The chloroform solution was washed with water and evaporated (3.4 mmol, 21%). ^{1}H NMR (270 MHz, $CDCl_3$) δ 4.07 (ddd, J = 5.7, 1.6, 1.6 Hz, 2H), 4.54 (s, 2H), 4.75 (s, 2H), 5.24 (ddt, J = 10.3, 1.6, 1.6 Hz, 1H), 5.32 (ddt, J = 10.3, 1.6, 1.6 Hz, 1H), 5.95 (m, 1H), 7.74 (t, J = 1.6 Hz, 1H), 8.50 (s, 1H), 8.51 (s, 1H).

4.2. Synthesis of 3-allyloxymethyl-5-chloromethylpyridine hydrochloride: ***6***

Compound **5** (1.93 mmol) was dissolved in 10 mL of chloroform and thionyl chloride (3.9 mmol) was added to this. The solution was refluxed for 1 h and then excess thionyl chloride was removed under vacuum to afford **5** (quantitatively). ^{1}H NMR (270 MHz, $CDCl_3$) δ 4.17 (ddd, J = 5.7, 1.4, 1.4 Hz, 2H), 4.74 (s, 2H), 4.81 (s, 2H), 5.28–5.40 (m, 2H), 5.94 (m, 1H), 8.43 (s, 1H), 8.81 (s, 1H), 8.91 (s, 1H).

4.3. Synthesis of (3-allyloxymethyl-5-pyridinium)methyltriphenylphosphoniumchloride hydrochloride: ***7***

Under a nitrogen atmosphere, **6** (6.3 mmol) and PPh_3 (13 mmol) were dissolved in 80 mL of dry DMF and the mixture was stirred for 3 h at 90 °C. The solvent was removed under vacuum and the residue was dissolved in small amount of chloroform. Then, benzene was added to precipitate the title compound (85%). ^{1}H NMR (270 MHz, $CDCl_3$) δ 3.97 (ddd, J = 5.7, 1.4, 1.4 Hz, 2H), 4.39 (s, 2H), 5.19–5.29 (m, 2H), 5.86 (m, 1H), 5.92 (d, J = 15 Hz, 2H), 7.74 (m, 15H), 7.94 (s, 1H), 8.22 (s, 1H), 8.50 (s, 1H).

4.4. Synthesis of 3-allyloxymethyl-5-((E)-2-ferrocenyl-ethenyl)pyridine: ***8***

Under a nitrogen atmosphere, **7** (0.55 mmol), ferrocenecarboaldehyde [32] (0.60 mmol) and sodium hydride (1.1 mmol) were added into 10 mL of dry DMF and the mixture was stirred for 3 h at room temperature. Small amount of water was added to quench the reaction and the solvent was removed under vacuum. The residue was extracted with chloroform and the title compound was purified using silica gel column chromatography (eluent: *n*-hexane/EtOAc = 5:1) (17%). ^{1}H NMR (270 MHz, $CDCl_3$) δ 4.09 (ddd, J = 7.0, 1.4, 1.4 Hz, 2H), 4.15 (s, 1H), 4.48 (t, J = 1.6 Hz, 2H), 4.55 (s, 2H), 5.26 (ddt, J = 10.5, 1.1, 1.1 Hz, 2H), 5.35 (ddt, J = 10.5, 1.1, 1.1 Hz, 2H), 6.06 (m, 1H), 6.66 (d, J = 16.5 Hz, 1H), 6.97 (d, J = 16.5 Hz, 1H), 7.76 (t, J = 2.2 Hz, 1H), 8.40 (d, J = 2.2 Hz, 1H), 8.55 (d, J = 2.2 Hz, 1H).

4.5. Synthesis of 3-allyloxymethyl-5-((E)-2-(4-formyl-phenyl)ethenyl)pyridine: ***9***

Under an argon atmosphere, **7** (0.18 mmol) was dissolved in 4 mL of dry DMF and potassium *tert*-butoxide (0.45 mmol) was added at −40 °C. After stirring for 10 min at 0 °C, terephthalaldehyde (0.73 mmol) was added and stirred for 2 h. After removal of solvent under vacuum, 50 mL of saturated aqueous solution of ammonium chloride was added and extracted with ether. The crude product was purified using flash silica gel column chromatography (eluent: ether) (20%). ^{1}H NMR (270 MHz, $CDCl_3$) δ 4.10 (dd, J = 5.7, 1.1 Hz, 2H), 4.58 (s, 2H), 5.27 (dd, J = 10, 1.4 Hz, 2H), 5.35 (dd, 2H, J = 10, 1.4 Hz, 2H), 5.98 (m, 1H), 7.24 (s, 2H), 7.68 (d, J = 8.1 Hz, 2H), 7.89 (s, 1H), 7.90 (d, J = 8.1 Hz, 2H), 8.49 (s, 1H), 8.68 (s, 1H), 10.02 (s, 1H).

4.6. Synthesis of 3-allyloxymethyl-5-((E)-2-(4-(N-octadecy-lfulleropyrrolidinyl)phenyl)ethenyl)pyridine: ***10***

N-Octadecylglycine (0.34 mmol), **9** (0.17 mmol), and fullerene (0.34 mmol) were mixed into 200 mL of toluene and refluxed for 8 h. After cooling to room temperature, the reaction solution was concentrated to a small volume and subjected to silica gel column chromatography (eluent: chloroform/acetone = 20:1) (64%). ^{1}H NMR (270 MHz, $CDCl_3$) δ 0.88 (t, J = 6.8 Hz, 3H), 1.25 (br, 30H), 1.95 (m, 2H), 2.58–3.23 (m, 2H), 4.07 (ddd, J = 5.7, 1.6, 1.6 Hz, 2H), 4.13 (d, J = 9.5 Hz, 1H), 5.08 (s, 1H), 5.11 (d, J = 9.5 Hz, 2H), 5.24 (dd, J = 10.3, 1.6 Hz, 2H), 5.33 (ddt, J = 17.3, 1.6, 1.6 Hz, 2H), 5.96 (m, 1H), 7.10 (d, J = 16.5 Hz, 2H), 7.19 (d, J = 16.5 Hz, 2H), 7.58 (d, J = 8.6 Hz, 2H), 7.83 (brs, 3H), 8.44 (s, 1H), 8.64 (s, 1H).

4.7. Synthesis of 5,15-bis(2-allyloxyethyl)porphyrin: ***11***

Under a nitrogen atmosphere, 2-allyloxy-1-propanal [33,34] (0.6 mmol) and dipyrromethane [35] (0.4 mmol) were dissolved in 100 mL of chloroform. Trifluoroacetic acid (TFA, 0.8 mmol) was added and the solution was stirred for 15 h at room temperature under dark. Chloranil (1.2 mmol) was then added to the reaction solution and stirred for further 12 h. The reaction mixture was washed with aqueous sodium bicarbonate, and the organic layer was evaporated. The crude product was purified using silica gel column chromatography (eluent: chloroform) (25%). MS (MALDI-TOF) found for $[M+1]^+$ 479.2, calcd. 478.2; ^{1}H NMR (270 MHz, $CDCl_3$) δ −3.04 (s, 2H), 4.09 (ddd, J = 5.4, 1.4, 1.4 Hz, 4H), 4.48 (t, J = 7.6 Hz, 4H), 5.16 (ddt, J = 10.4, 1.4, 1.4 Hz, 2H), 5.28 (m, 6H), 5.96 (m, 2H), 9.38 (d, J = 4.6 Hz, 4H), 9.58 (d, J = 4.6 Hz, 4H), 10.13 (s, 2H).

4.8. Synthesis of 5,15-bis(2-allyloxyethyl)-10-iodoporphyrin: **12**

To a solution of porphyrin **11** (0.105 mmol) in 250 mL of chloroform was added dropwise a mixture of bis(trifluoroacetoxy)iodobenzene (0.078 mmol), iodine (0.063 mmol), and pyridine (0.5 mmol) in 25 mL of chloroform over 1 h. The reaction solution was washed with saturated aqueous solution of sodium thiosulfate. The crude product was purified using flash silica gel column chromatography (eluent: chloroform/acetone = 20:1) (35%). MS (MALDI-TOF) found for $[M+1]^+$ 605.1, calcd. 604.1; ^{1}H NMR (270 MHz, $CDCl_3$) δ −3.01 (s, 2H), 4.10 (ddd, J = 5.4, 1.4, 1.4 Hz, 4H), 4.47 (t, J = 7.8 Hz, 4H), 5.17–5.32 (m, 8H), 5.90 (m, 2H), 9.33 (d, J = 4.9 Hz, 4H), 9.53–9.57 (m J = 4.9 Hz, 4H), 10.06 (s, 1H).

4.9. Synthesis of 5-(5′,15′-bis(allyloxyethyl)porphyrinylethyn-2-yl)-10,15-bis(methoxycarbonylethyl)-20-(l-methyl-2-imidazolyl)porphyrin: **13**

Under a nitrogen atmosphere, porphyrin **12** (0.13 mmol), 5-ethynyl-10,20-bis(methoxycarbonylethyl)-15-(l-methyl-2-imidazolyl)porphyrin [21] (0.11 mmol), tris(dibenzylideneacetone)dipalladium (0) (0.0176 mmol) and triphenylarsine (0.14 mmol) were dissolved in a mixture of dry THF (17.5 mL) and triethylamine (3.5 mL). After stirring for 5 h at 40 °C, the solvent was removed under vacuum and the residue was extracted with chloroform. The crude product was purified using flash silica gel column chromatography (eluent: chloroform/acetone = 5:1) (95%). MS (MALDI-TOF) found for $[M+1]^+$ 1063.7, calcd. 1062.5; ^{1}H NMR (270 MHz, $CDCl_3$) δ −3.40 (s, 2H), −3.59 (s, 2H), 4.43–4.41 (m, 7H), 3.80 (s, 6H), 4.12 (d, 4H), 4.39 (t, J = 12 Hz, 4H), 4.99–5.08 (m, 8H), 5.21 (dd, J = 10.5, 1.2 Hz, 2H), 5.33 (dd, J = 17.4, 1.8 Hz, 2H), 6.00 (m, 2H), 7.56 (s, 1H), 7.85 (s, 1H), 8.80 (d, J = 1.6 Hz, 2H), 8.97 (d, J = 1.6 Hz, 2H), 9.09 (d, J = 1.6 Hz, 2H), 9.19 (d, J = 1.6 Hz, 2H), 9.36 (m, J = 1.6 Hz, 2H), 9.49 (s, 1H), 9.63 (d, J = 1.6 Hz, 2H), 10.02 (d, J = 1.6 Hz, 2H), 10.45 (d, J = 1.6 Hz, 2H).

4.10. Synthesis of 5-(5′,15′-(bis-allyloxyethyl)porphyrinylethyn-2-yl)-10,15-bis(allyloxycarbonylethyl)-20-(l-methyl-2-imidazolyl)porphyrin: **14**

Porphyrin **13** (0.105 mmol), allylalcohol (90.9 mmol), and 1,3-dichlorotetrabutyldistannoxane [36] (2.08 mmol) were dissolved in 130 mL of toluene. After refluxing for 20 h at 70 °C, solvent was removed under vacuum and the residue was extracted with chloroform. The crude product was purified using silica gel column chromatography (eluent: chloroform/acetone = 5:1) (68%). MS (MALDI-TOF) found for $[M+1]^+$ 1115.8, calcd. 1114.5; ^{1}H NMR (270 MHz, $CDCl_3$) δ −3.99 (s, 2H), −3.79 (s, 2H), 3.39 (br, 7H), 4.09 (d, J = 5.4 Hz, 4H), 4.33 (t, J = 7.8 Hz, 4H), 4.74 (d, 4H), 5.10–4.90 (br, 8H), 5.29 (m, 8H), 5.96 (m, 4H), 7.56 (d, J = 1.4 Hz, 1H), 7.88 (d, J = 1.4 Hz, 1H), 8.80 (d, J = 1.6 Hz, 2H), 8.84 (d, J = 1.6 Hz, 2H), 8.93 (d, J = 1.6 Hz, 2H), 9.03 (d, J = 1.6 Hz, 2H), 9.29–9.34 (m, 3H), 9.58 (d, J = 1.6 Hz, 2H), 9.88 (d, J = 1.6 Hz, 2H), 10.43 (d, J = 1.6 Hz, 2H).

4.11. Synthesis of 5-(5′,15′-(bis-allyloxyethyl)porphyrinatozinc(II)ethyn-2-yl)-10,15-bis(allyloxycarbonylethy)-20-(l-methyl-2-imidazolyl)porphyrinatozinc(II): **15**

To a solution of free base porphyrin **14** (0.072 mmol) in 200 mL of chloroform was added a saturated solution of zinc acetate dihydrate (7.2 mmol) in methanol. After stirring for 2 h at room temperature, the reaction solution was washed with water and then evaporated. The residue was once dissolved in a small amount of chloroform and then methanol was added to allow precipitation of the product, which was found to be the stacked form of the target compound **15st** (stack) as the major product (88%). MS (MALDI-TOF) found for $[M+1]^+$ 1241.3, calcd. 1240.3 (detected as a monomeric form); ^{1}H NMR (270 MHz, $CDCl_3$) δ 1.88 (s, 6H), 2.12 (s, 2H), 4.31 (m, 8H), 4.48 (t, J = 5.3 Hz, 8H), 4.85 (m, 8H), 5.14 (m, 8H), 5.42 (d, J = 9.1 Hz, 4H), 5.50 (d, 4H, J = 9.1 Hz), 5.56 (br 8H), 5.58 (dd, J = 16.9, 1.1 Hz, 4H), 5.62–5.63 (m, 4H), 5.68 (dd, J = 16.9, 1.1 Hz), 5.80 (s, 8H), 6.28–6.36 (m, 8H), 7.66 (d, J = 3.6 Hz, 4H), 7.86 (d, J = 3.6 Hz, 4H), 9.20 (d, J = 3.6 Hz, 4H), 9.43 (d, J = 3.6 Hz, 4H), 9.50 (d, J = 3.6 Hz, 4H), 9.66 (d, J = 3.6 Hz, 4H), 9.74 (d, J = 3.6 Hz, 4H), 10.22 (s, 2H).

4.12. Synthesis of **4b**

Self-assembled product **15st** (1.36 μmol) was once dissolved in 20 mL of pyridine and then dried up to be converted to the extended isomer **4a** as the major species (94%). The residue was dissolved in 6.8 mL of tetrachloroethane and the Grubbs catalyst ($RuCl_2$(=CH-p-C_6H_5)(PCy_3)$_2$, 1.1 μmol) was added. The reaction solution was stirred for 4 h at 0 °C under a nitrogen atmosphere and dark. The solvent was then removed under vacuum and the residue was extracted with chloroform. The crude product was purified using silica gel column chromatography (eluent: chloroform/methanol = 10:1) to yield the covalently fixed extended isomer **4b** (73%) free from the stacked isomer. MS (MALDI-TOF) found for $[M+1]^+$ 2428.7, calcd. 2427.6; ^{1}H NMR (270 MHz, $CDCl_3$) δ 1.84 (s, 6H), 2.43 (s, 2H), 3.99–3.85 (br, 8H), 4.22 (d, J = 5.4 Hz, 8H), 4.65 (s, 8H), 5.09 (m, 8H), 5.13 (d, J = 10.2 Hz, 4H), 5.38 (d, J = 10.2 Hz, 4H), 5.46 (br 8H), 5.56 (br 8H), 5.62 (d, J = 3.6 Hz, 4H), 5.67 (s, 2H), 6.05 (m, 2H), 6.44 (s) 6.51 (s), 8.99–9.01 (br, 4H), 9.39 (d, J = 3.6 Hz, 4H), 9.70 (d, J = 3.6 Hz, 4H), 9.92–9.95 (m, 4H), 9.99 (d, J = 3.6 Hz, 4H), 10.13 (s, 2H), 10.72 (d, J = 3.6 Hz, 4H), 10.73 (d, J = 3.6 Hz, 4H).

4.13. Synthesis of FcFc

Under a nitrogen atmosphere, **4b** (5.6 μmol) and **7** (16.8 μmol) were dissolved in 11 mL of tetrachloroethane and the Grubbs catalyst (11.2 μmol) was added. The reaction solution was stirred for 5 h at 0 °C under dark. The solvent was removed under vacuum and the residue was extracted with chloroform. The target compound was isolated by silica gel

column chromatography (eluent: benzene/THF = 7:1 (5.8%). MS (MALDI-TOF) found for $[M]^+$ 3089.0 calcd. 3089.7; ^{1}H NMR (270 MHz, $CDCl_3$) δ 1.83 (s, 6H), 2.35, 2.37 (2s, 2H), 2.43, 2.45 (2d, J = 1.8 Hz, 2H), 2.46 (s, 2H), 3.22, 3.24 (2s, 4H), 3.27 (d, J = 12 Hz), 3.38 (s), 3.83 (d, J = 6.6 Hz), 3.85–3.99 (br, 8H), 4.08 (s), 3.80–4.10 (br, 8H), 4.04, 4.05 (2s), 4.19–4.25 (m, 12H), 4.29, 4.31 (2t, J = 6.0 Hz, 4H), 4.52, 4.57 (2t, J = 6.0 Hz, 4H), 4.76 (t, J = 7.2 Hz, 4H), 5.11 (d, J = 10.8 Hz, 8H), 5.38 (d, J = 10.8 Hz, 4H), 5.30, 5.31 (2d, J = 10.8 Hz), 5.43–5.61 (m), 5.62 (d, J = 3.6 Hz, 4H), 5.68 (s, 1H), 5.75, 5.77 (2d, J = 10.8 Hz, 1H), 5.92–5.88 (m), 6.13 (m, 2H), 6.27, 6.30 (2s), 6.46 (s), 6.54 (s), 9.01 (br, 4H), 9.39, 9.40 (2d, J = 4.2 Hz, 4H), 9.42, 9.44 (2d, J = 4.2 Hz, 4H), 9.69, 9.72 (2d, J = 4.2 Hz, 4H), 9.76, 9.77 (2d, J = 4.2 Hz, 4H), 9.88–9.91 (m, 4H), 9.88, 9.97 (2d, J = 4.2 Hz, 2H), 10.04–10.06 (m, 4H), 10.76, 10.80 (2d, J = 4.2 Hz).

4.14. Synthesis of $C_{60}C_{60}$

Under a nitrogen atmosphere, **4b** (3.7 μmol) and **9** (7.4 μmol) were dissolved in 5 mL of tetrachloroethane and the Grubbs catalyst (7.3 μmol) was added. The reaction solution was stirred for 2 h at room temperature under dark. The solvent was removed under vacuum and the residue was extracted with chloroform. The target compound was isolated by silica gel column chromatography (eluent: chloroform/acetone = 50:1) (13%). The byproduct of mono-C_{60} substituted compound was isolated in this stage and used for the preparation of **C_{60}Fc**. MS (MALDI-TOF) found for $[M]^+$ 4903.0, calcd. 4902.4; ^{1}H NMR (270 MHz, $CDCl_3$) δ 0.85 (t, 6H), 1.25–3.09 (br, 66H), 1.87 (s, 6H), 2.35, 2.39 (2s, 2H), 2.51, 2.54 (2d, J = 1.8 Hz, 2H), 2.45 (br, 2H), 3.23 (br), 3.40 (s), 3.80–4.10 (br, 12H), 4.24 (m, 4H), 4.50–4.55 (br, 4H), 4.71 (br, 4H), 4.90 (s, 2H), 4.98 (d, J = 7.8 Hz, 2H), 5.11 (d, J = 10.8 Hz, 8H), 5.23 (d, J = 10.8 Hz, 2H), 5.38 (d, J = 10.8 Hz, 2H), 5.43–5.61 (m, 16H), 5.63 (br, 4H), 5.71 (d, 2H), 5.94 (d, J = 16 Hz, 2H), 6.07 (m, 2H), 6.35, 6.36 (2s), 6.48 (s), 6.55 (s), 9.01 (br, 4H), 9.39 (br, 4H), 9.42, 9.69, 9.72 (br, 4H), 9.88–9.90 (m, 4H), 9.93 (br, 2H), 10.03–10.05 (m, 4H), 10.72–10.78 (br).

4.15. Synthesis of $C_{60}Fc$

Under a nitrogen atmosphere, mono-C_{60} substituted compound, which was obtained in the synthesis of **$C_{60}C_{60}$** (1.36 μmol), and **8** (2.0 μmol) were dissolved in 5 mL of tetrachloroethane and the Grubbs catalyst (1.36 μmol) was added. The reaction solution was stirred for 2 h at room temperature under dark. The solvent was removed under vacuum and the residue was extracted with chloroform. The target compound was isolated by silica gel column chromatography (eluent: chloroform/acetone = 50:1) (∼1 mg). MS (MALDI-TOF) found for $[M]^+$ 3997.1, calcd. 3996.0.

5. Measurement of non-linear absorption

Nanosecond open-aperture Z-scan measurements were undertaken by using an optical parametric oscillator (Continuum Surelight OPO) pumped with a THG beam from a Q-switched Nd:YAG laser (Continuum Surelight I-10) ranged from 770 nm to 940 nm. The pulse width and the repetition rate were 5 ns and 10 Hz, respectively. The laser beam was focused using a plano-convex lens (f = 100 mm) with a beam waist of around 0.035 mm at the focal point. The Z-scan measurement was undertaken for rhodamin B in a methanol solution and the cross-section value was found to be 21 GM at 1064 nm, which was comparable to the reported value of 14.3 GM measured by the fluorescence method at 1064 nm [37].

Acknowledgments

This work was supported by Grant-in-Aids for Scientific Research (A) (No. 15205020) and for Exploratory Research (No. 16655072) from Ministry of Education, Culture, Sports, Science and Technology, Japan (Monbu Kagakusho), and by Iketani Science Technology Foundation. K.O. acknowledges partial financial support from Kinki-Chiho Invention Center.

References

[1] J.D. Bhawalkar, N.D. Kumar, C.F. Zhao, P.N. Prasad, J. Clin. Laser Med. Surg. 15 (1997) 201.
[2] E.A. Wachter, W.P. Partridge, W.G. Fisher, H.C. Dees, M.G. Petersen, Proc. SPIE-Into. Soc. Opt. Eng. 3269 (1998) 68.
[3] J. Liu, Y.W. Zhao, J.Q. Zhao, A.D. Xia, L.J. Jiang, S. Wu, L. Ma, Y.Q. Dong, Y.H.J. Gu, Photochem. Photobiol. B 68 (2002) 156.
[4] D.A. Parthenopoulos, P.M. Rentzepis, Science 245 (1989) 843.
[5] J.H. Strickler, W.W. Webb, Opt. Lett. 16 (1991) 1780.
[6] Y. Shen, C.S. Friend, Y. Jiang, D. Jakubczyk, J. Swiatkiewicz, P.N. Prasad, J. Phys. Chem. B 104 (2000) 7577.
[7] A.S. Dvornikov, Y. Liang, C.S. Cruse, P.M. Rentzepis, J. Phys. Chem. B 108 (2004) 8652.
[8] H.S. Nalwa, S. Miyata (Eds.), Nonlinear Optics of Organic Molecules and Polymers, CRC Press, Boca Raton, FL, 1997.
[9] M. Göppert-Mayer, Ann. Phys. 9 (1931) 273.
[10] W. Kaiser, C.G.B. Garret, Phys. Rev. Lett. 7 (1961) 229.
[11] M. Albota, D. Beljonne, J.-L. Brédas, J.E. Ehrlich, J.-Y. Fu, A.A. Heikal, S.E. Hess, T. Kogej, M.D. Levin, S.R. Marder, D. McCord-Maughon, J.W. Perry, H. Röckel, M. Rumi, G. Subramaniam, W.W. Webb, X.-L. Wu, C. Xu, Science 281 (1998) 1653.
[12] B.A. Reinhardt, L.L. Brott, S.J. Clarson, A.G. Dillard, J.C. Bhatt, R. Kannan, L. Yuan, G.S. He, P.N. Prasad, Chem. Mater. 10 (1998) 1863.
[13] M. Drobizhev, A. Karotki, M. Kruk, A. Rebane, Chem. Phys. Lett. 355 (2002) 175.
[14] R.W. Waynant, M.N. Ediger (Eds.), Electro-Optics Handbook, McGraw-Hill, New York, 1993 (Chapter 24).
[15] Y. Kobuke, H. Miyaji, J. Am. Chem. Soc. 116 (1994) 4111.
[16] Y. Kobuke, K. Ogawa, Bull. Chem. Soc. Jpn. 76 (2003) 689.
[17] K. Ogawa, Y. Kobuke, Angew. Chem. Int. Ed. 39 (2000) 4070.
[18] K. Ogawa, T. Zhang, K. Yoshihara, Y. Kobuke, J. Am. Chem. Soc. 124 (2002) 22.
[19] R. Takahahshi, Y. Kobuke, J. Am. Chem. Soc. 125 (2003) 2372.
[20] K. Ogawa, A. Ohashi, Y. Kobuke, K. Kamada, K. Ohta, J. Am. Chem. Soc. 125 (2003) 356.
[21] A. Ohashi, A. Satake, Y. Kobuke, Bull. Chem. Soc. Jpn. 77 (2004) 365.
[22] V.S.-Y. Lin, S.G. DiMagno, M.J. Therien, Science 264 (1994) 1105.
[23] H.L. Anderson, Chem. Commun. (1999) 2323.
[24] P.N. Taylor, A.P. Wylie, J. Huuskonen, H.L. Anderson, Angew. Chem. Int. Ed. 37 (1998) 986.
[25] K. Kamada, K. Ohta, Y. Iwase, K. Kondo, Chem. Phys. Lett. 372 (2003) 386.
[26] P. Audebert, K. Kamada, K. Matsunaga, K. Ohta, Chem. Phys. Lett. 367 (2003) 62.

[27] L. Antonov, K. Kamada, K. Ohta, S. Kamounah, Phys. Chem. Chem. Phys. 5 (2003) 1193.
[28] J. Swiatkiewicz, P.N. Prasad, B.A. Reinhardt, Opt. Commun. 157 (1998) 135.
[29] O.-K. Kim, K.-S. Lee, H.Y. Woo, K.-S. Kim, G.S. He, J. Swiatkiewicz, P.N. Prasad, Chem. Mater. 12 (2000) 284.
[30] H. Lei, H.Z. Wang, Z.C. Wei, X.J. Tang, L.Z. Wu, C.H. Tung, G.Y. Zhou, Chem. Phys. Lett. 333 (2001) 387.
[31] K. Tsuda, N. Ikekawa, R. Takasaki, Y. Yamakawa, Chem. Pharm. Bull. (1953) 142.
[32] G.G.A. Balavoine, G. Doisneau, T. Fillebeen-Khan, J. Organomet. Chem. 412 (1991) 381.
[33] I. Kadota, M. Kawada, V. Gevorgyan, Y. Yamamoto, J. Organomet. Chem. 62 (1997) 7439.
[34] A.J. Mancuso, S.-L. Huang, D. Swern, J. Organomet. Chem. 43 (1978) 2480.
[35] Q.M. Wang, D.W. Bruce, Synlett (1995) 1267.
[36] J. Otera, N. Danoh, H. Nozaki, J. Organomet. Chem. 56 (1991) 5307.
[37] J.P. Hermann, J. Ducuing, Opt. Commun. 6 (1972) 101.